NASA

Technical Memorandum **78029**

SYSTEMS FOR MEASURING THE RESPONSE STATISTICS OF GIGAHERTZ BANDWIDTH PHOTOMULTIPLIERS

J. B. Abshire and H. E. Rowe

DECEMBER 1977

National Aeronautics and
Space Administration

Goddard Space Flight Center
Greenbelt, Maryland 20771

BIBLIOGRAPHIC DATA SHEET

1. Report No.	2. Government Accession No.	3. Recipient's Catalog No.
TM-78029		

4. Title and Subtitle	5. Report Date
Systems for Measuring Response Statistics of Gigahertz Bandwidth Photomultipliers	December 1977
	6. Performing Organization Code 723
7. Author(s) James B. Abshire and H. Edward Rowe	8. Performing Organization Report No. G7703-X31
9. Performing Organization Name and Address Goddard Space Flight Center Greenbelt, Maryland 20771	10. Work Unit No. 506-20-33
	11. Contract or Grant No.
	13. Type of Report and Period Covered Technical Memorandum
12. Sponsoring Agency Name and Address National Aeronautics and Space Administration Washington, D.C. 20546	14. Sponsoring Agency Code

15. Supplementary Notes

To be published in "Review of Scientific Instruments."

16. Abstract

New systems have been developed for measuring the average impulse response, the pulse-height spectrum, the transit-time statistics as a function of signal level, and the dark-count spectrum of gigahertz bandwidth photomultipliers. Measurements showed that the 0.53-μm pulse used as an optical test source had a 30-ps rise time and less than 70-ps pulse width. Calibration data showed the system resolution to be less than 20 ps for rms transit-time measurements. Test data for a static crossed-field photomultiplier showed 2-photoelectron resolution and less than 30-ps time jitter over the 1- to 100-photoelectron range.

17. Key Words (Selected by Author(s))	18. Distribution Statement
Photomultiplier measurement system, High-speed photomultipliers, Waveform analysis, Photomultiplier transit-time statistics, Static crossed-field photomultiplier	STAR Category 35 Unclassified–Unlimited

19. Security Classif. (of this report)	20. Security Classif. (of this page)	21. No. of Pages	22. Price*
Unclassified	Unclassified	30	$4.50

*For sale by the National Technical Information Service, Springfield, Virginia 22151.

All measurement values are expressed in the International System of Units (SI) in accordance with NASA Policy Directive 2220.4, paragraph 4.

SYSTEMS FOR MEASURING THE RESPONSE STATISTICS OF GIGAHERTZ BANDWIDTH PHOTOMULTIPLIERS

James B. Abshire and H. Edward Rowe

Introduction

Photomultipliers have been used in precise optical detection and timing applications for many years due to their high sensitivity and fast response times. These applications include subnanosecond fluorescence spectroscopy,[1] optical communications,[2] and laser ranging.[3] Recent advances in laser and photomultiplier technologies have led to lasers with output pulse widths of less than 50 picoseconds (ps) and photomultipliers with bandwidths in excess of 3 GHz.[4] The increasing use of short pulsed lasers in optical detection and timing applications makes the characterization of photomultipliers used with these optical sources mandatory.

This document describes measurement systems developed at the Goddard Space Flight Center (GSFC) for measuring four of the most important photomultiplier response characteristics at 0.53 μm. These measurements include the average impulse response, the pulse height spectrum, the mean and root mean squared electron transit times as a function of signal level, and the noise

pulse-amplitude spectrum of the photomultiplier. The first three measurements utilize a fast transient digitizer and minicomputer data processing. The timing system can resolve less than 20-ps (rms) time jitter and mean transit time changes of less than 15 ps.

Many components of these systems were developed for GSFC's high-data-rate, short-pulse laser data-relay program* and now are used in laboratory devices to support component development for GSFC's laser ranging program.[5†] Test results from evaluating seven photomultipliers using these systems has been recently published.[6]

Measurements show that the 0.53-μm pulse used as an optical test source has less than 50-ps rise time and less than 70-ps pulse width. Calibration data showed the system resolution to be less than 20 ps for rms transit-time measurements.

Typical test data for a static crossed-field photomultiplier showed less than 30-ps rms time jitter over the 1- to 100-photoelectron range. Measurements

---

*M. Fitzmaurice, "Laser Data Relay Link Program," NASA/GSFC Internal Publication, August 1973.

†M. W. Fitzmaurice, P. O. Minott, and W. D. Kahn, "Development and Testing of a Spaceborne Laser Ranging System Engineering Model," NASA/GSFC X-723-75-307, November 1975.

of the dark-count spectra for the same detector show little change in the distribution of dark counts with average anode current for signals above 1 photoelectron.

Average Impulse Response Measurement System

Figure 1 shows the system used to measure the average impulse response of optical detectors. Short 1.06-μm pulses are generated at a 400-Mpps rate from a mode-locked Nd:YAG (neodymium yttrium aluminum garnet) laser[7] and directed into a high-speed 1.06-μm modulator.[8] A fraction of the 200-MHz drive to the laser's acousto-optic mode-locker was diverted to a 2×10^7 count-down circuit. The circuit, which was built at GSFC of standard MECL-III components, outputs a square-wave pulse 10^4 times per second synchronously with the laser mode-locked pulses. Part of the pulse energy is used to trigger a sampling timebase, while the remainder is differentiated by a small capacitor. This differentiation results in a 2-ns-wide voltage spike at the leading and trailing edges of each square-wave pulse. The resulting pulse train is delayed by a delay box and serves as the signal source for the electro-optic modulator.

The electro-optic modulator only triggers on the negative-going spikes from the signal input, and therefore only gates out laser pulses at a rate of 10^4 pulses per second. The remaining pulses are attenuated by a factor of 20 or more by the modulator. The gated laser pulses are directed into a nonlinear optical crystal, where approximately 1 percent of the incoming 1.06-μm radiation is converted to 0.53 μm.

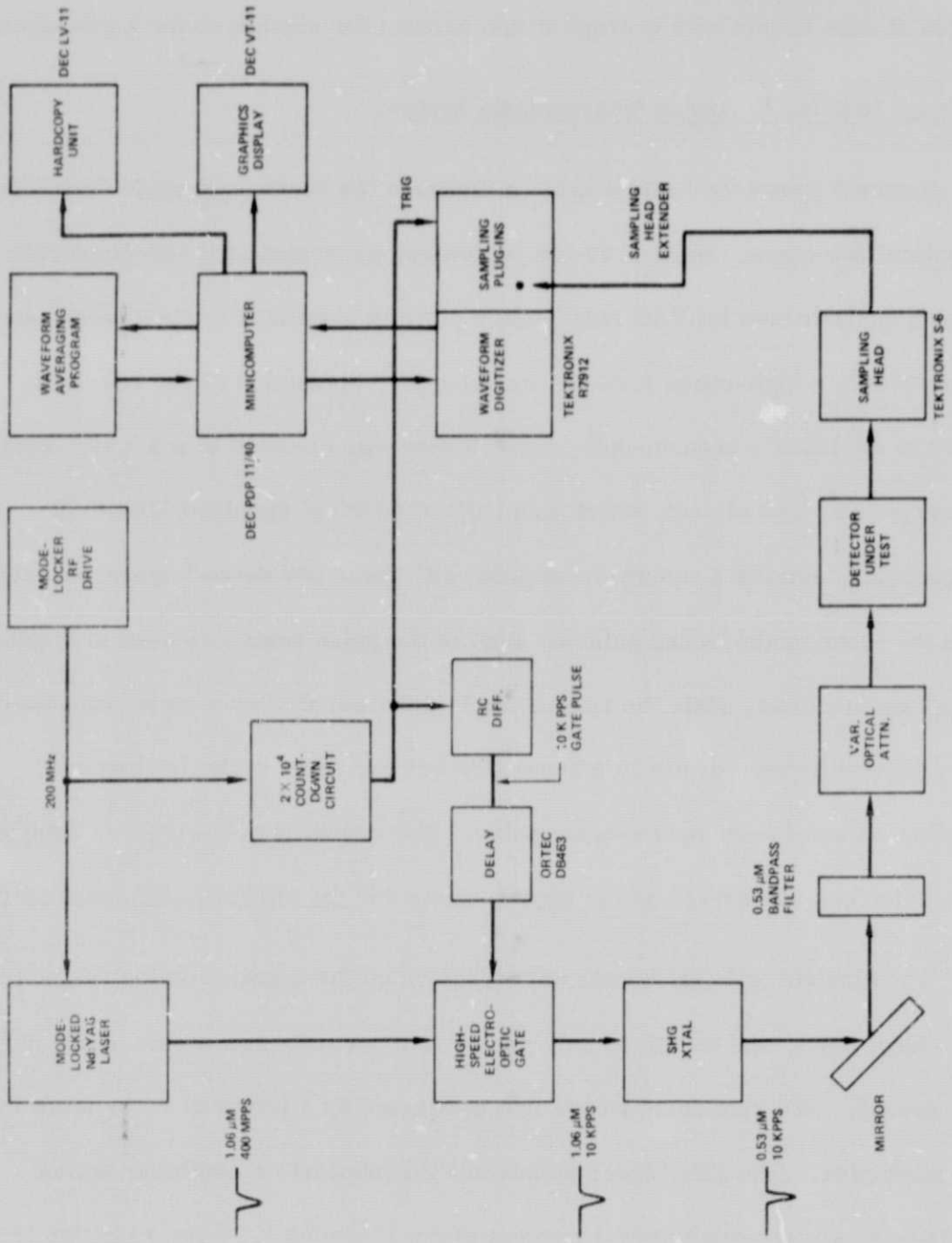

Figure 1. Block Diagram of System for Measuring Detector Average Impulse Response

The 1.06- and 0.53-μm pulses are then directed into a mirror and a 0.53-μm bandpass filter, which passes only the 0.53-μm pulses. These pulses are then directed through a stack of optical attenuators to the detector under test. The optical beam is focused at this point and has a spot size of 2 mm or less.

The electrical output of the detector is coupled directly to a sampling head, with no intervening cable to degrade the detector pulse risetime. The sampling-head signal goes through a sampling-head extender to the sampling vertical amplifier, which is mounted with the sampling timebase in a transient digitizer. The sampled and digitized waveforms are then read and processed under program control by a minicomputer.

The computer averages typically 100 sampled waveforms to reduce the sampling noise inherent in the sampling oscilloscope. The averaged waveform is then displayed on the minicomputer graphics display and optionally hard-copied on an electrostatic printer-plotter.

In testing the speed or response of fast electro-optic or electronic devices, the finite risetimes of the signal source and measuring devices must be considered. For an electronic system consisting of a series combination of a pulse generator, an amplifier, and an oscilloscope, the observed risetime is related to the risetimes of the various units by:

$$\tau_{r\,(\text{observed})} \approx 1.1 \sqrt{\tau r^2_{(\text{generator})} + \tau r^2_{(\text{amplifier})} + \tau r^2_{(\text{oscilloscope})}} \qquad (1)$$

This equation is usually accurate to within 10 percent.[9]

Figure 2 shows the average pulse shape of the detected 1.06-μm laser pulse. This measurement was made by removing the optical bandpass filter and detecting the 1.06-μm laser pulses with an ultrafast avalanche photodiode (APD). The risetime calculated for this detector is less than 30 ps.[10] Figure 2 shows the combined risetimes of the 1.06-μm laser pulse, detector, and sampling oscilloscope to be 65 ps, with the measured pulse full width at half maximum (FWHM) to be 100 ps. By using equation 1 and assuming that the sampling oscilloscope and APD each have risetimes of 30 ps, the risetime of the 1.06-μm laser pulse can be calculated to be approximately 40 ps.

Available instrumentation does not permit direct measurement of the 0.53-μm pulse shape. However, its pulse shape can be calculated, because, for low incident powers, the instantaneous second harmonic power from the nonlinear optical crystal is proportional to the square of the instataneous incident power.[11, 12]

Figure 3 shows the calculated 0.53-μm pulse shape and shows a risetime of 50 ps and a width of 70 ps FWHM. Since the measured 1.06-μm waveshape was broadened by the measuring system before the 0.53-μm pulse shape was computed, the actual 0.53-μm pulse shape is narrower than that shown in figure 3. By using the corrected risetime of the 1.06-μm pulse as a basis for calculations, the actual risetime of the 0.53-μm pulse can be calculated to be approximately 30 ps.

The average pulse response of a high-speed static-crossed field photomultiplier (Varian 154 A/1.6L) is shown in figure 4 as a typical test result. By using

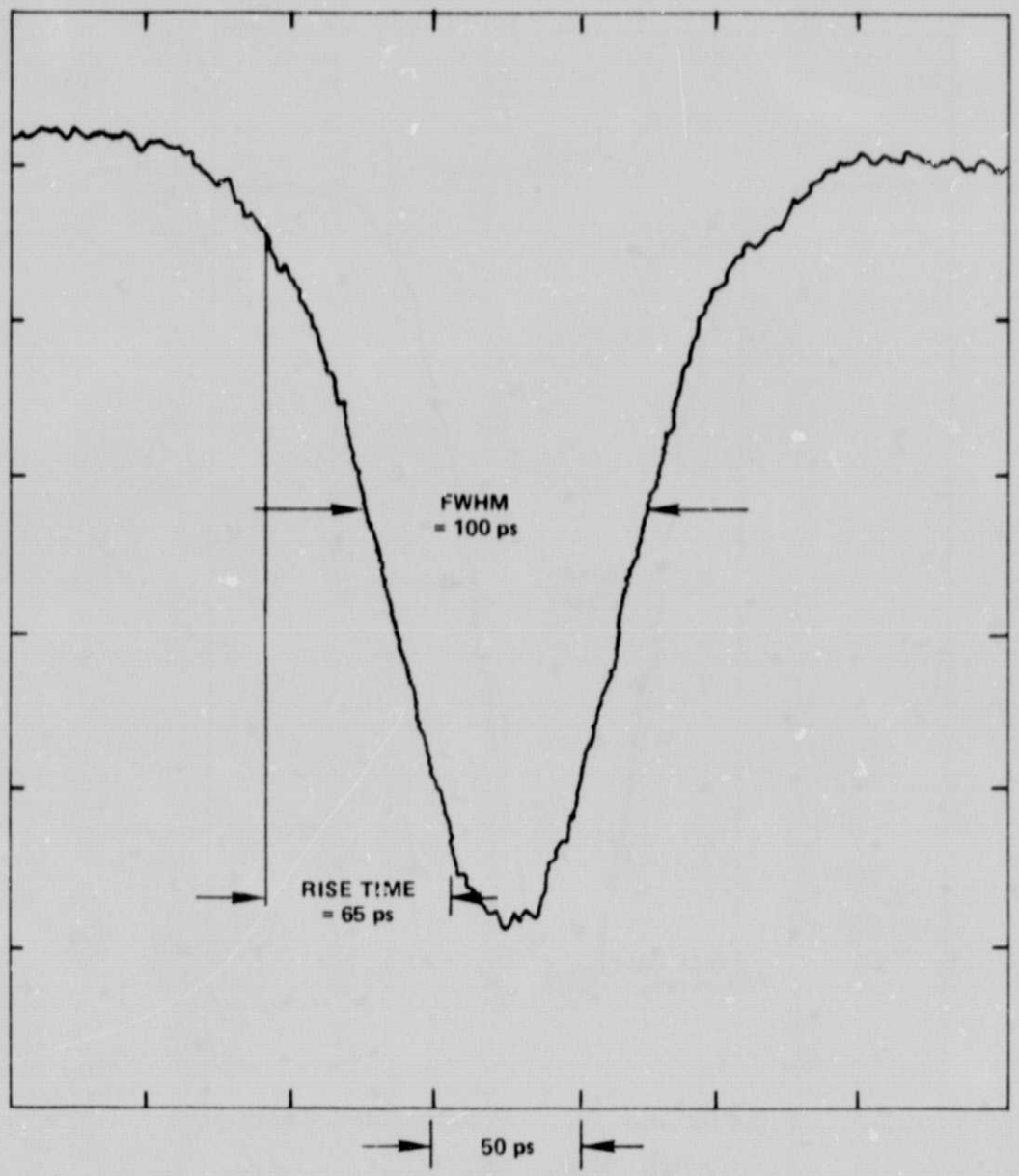

Figure 2. Measured 1.06-μm Pulse Shape

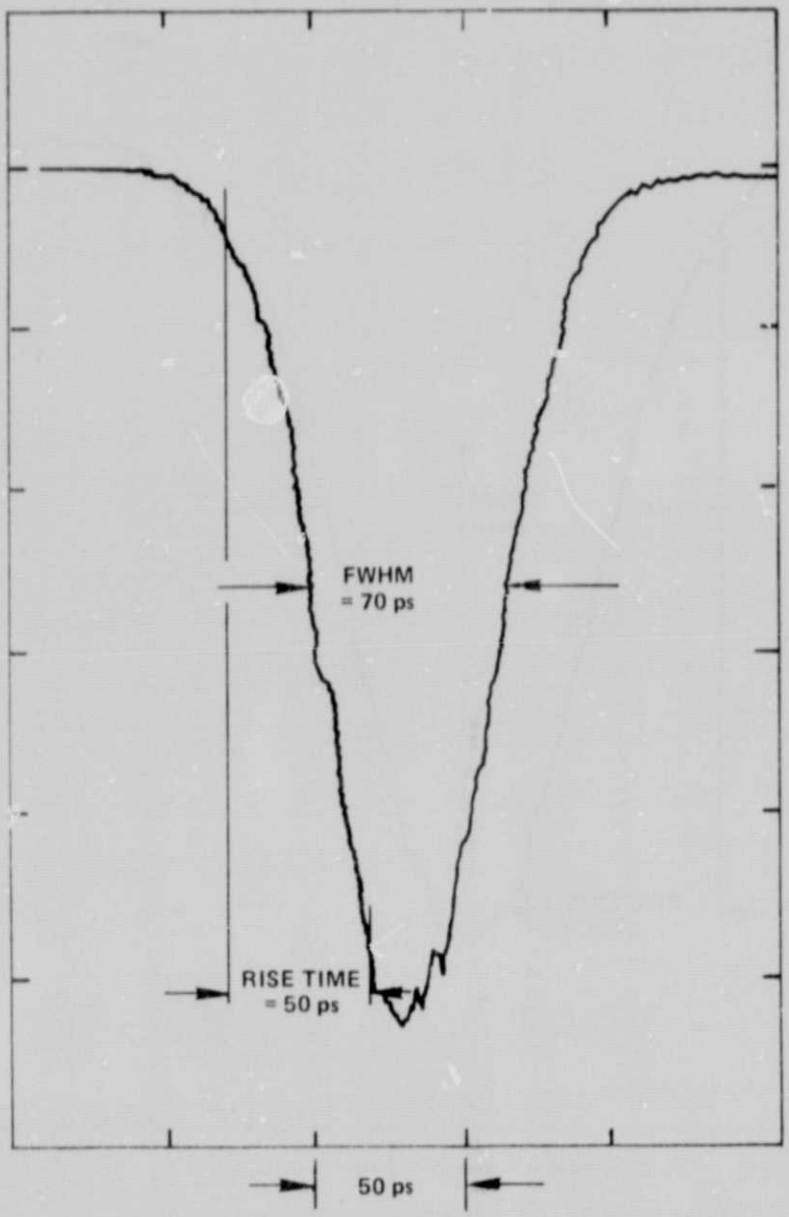

Figure 3. Calculated 0.53-μm Pulse Shape

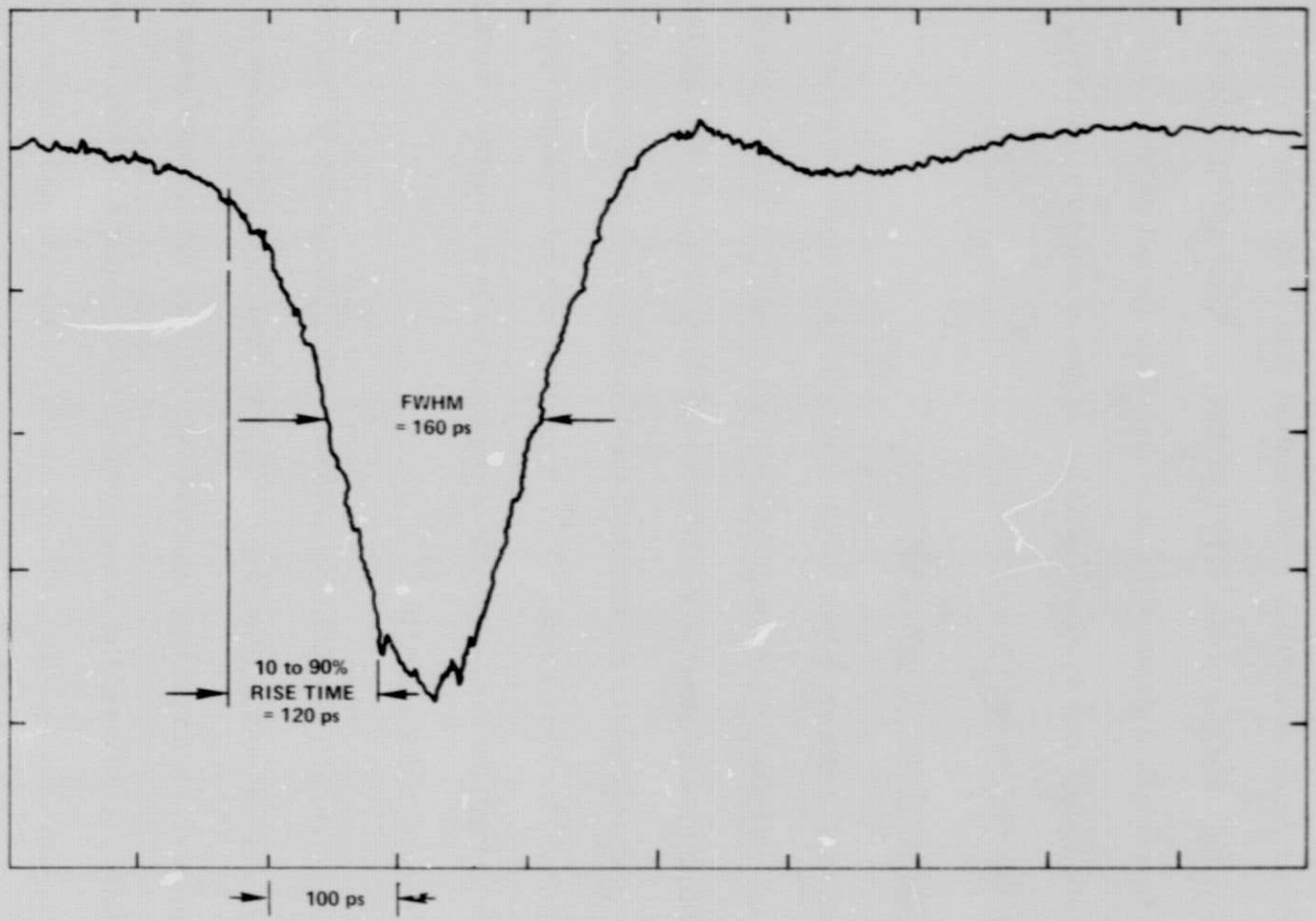

Figure 4. Varian 154 A/1.6L Average Pulse Response

equation 1 and assuming a laser pulse risetime of 30 ps and an instrumentation risetime of 30 ps, the computed risetime for this detector is 100 ps. Since the risetime of the pulse shown is degraded less than 10 percent, the pulse shown is effectively the response of this very fast detector to an optical impulse. Since the static crossed-field photomultiplier is one of the fastest photomultipliers presently available,[4] this system should be capable of measuring the response of all available high-speed photomultipliers.

Pulse-Height Spectrum Measurement System

The shape of a photomultiplier's pulse-height spectrum is essentially determined by the secondary emission gain of its first dynode. The development of dynodes with high-gain secondary emitters such as cesium-activated gallium phosphide (GaP(cs)) has culminated with the development of photomultipliers with up to 5-photoelectron resolution.[13, 14] Since then, the pulse-height resolution of these photomultipliers has become an active topic for both statistical modeling and experimental measurements.[15-20]

In most of the pulse-height measurements referenced above, the detector under test is either weakly illuminated with a dc continuous light source or short light pulse from a commercially available light pulser. Each output from the photomultiplier is directed into a multichannel pulse-height analyzer, where the count for the measured input channel number is incremented. Increasing channel numbers in the multichannel analyzer correspond to increasing peak

pulse amplitudes from the photomultiplier. For photomultipliers with low gains, the output pulse is sometimes preamplified before the multichannel analyzer. Commercial multichannel analyzers cannot directly analyze input pulses with widths less than 250 ns, and therefore must be used with pulse-shaping amplifiers for testing fast photomultipliers. It is doubtful whether this technique is suitable for use with static crossed-field photomultipliers, because no pulse-height spectra for these very fast detectors have been published.

A technique for measuring the pulse-height spectra of ultra fast photomultipliers and typical experimental results for a static crossed-field photomultiplier will be presented in this section. The experimental system is shown in figure 5. The laser, modelock drive, electro-optic gate, nonlinear optical crystal, optical bandpass filter, and variable optical attenuator are identical to those used in figure 1. However, the MECL-III countdown circuit was modified to divide the incoming 200 MHz by 2×10^7 by adding three additional divide-by-ten stages. This results in gating only ten optical pulses per second through the electro-optic gate. These pulses are frequency doubled, attenuated, and focused onto the photocathode of the detector under test, as was described earlier. The electrical output of the detector is sent through a wideband radio-frequency (RF) step attenuator, a Schottky diode pulse limiter, and two RF amplifiers. The purpose of the pulse limiter is to prevent any large ion-induced noise pulses from the photomultiplier from damaging the post-detection electronics. Pulses with

amplitude in excess of 200 mV are limited; all pulses with peak signals below this voltage are passed through undistorted. As can be seen from the bandwidths for each component listed in figure 5, the effective bandwidth of the amplifier chain is limited by the last amplifier to 1 MHz through 1.5 GHz.

The amplified signal is received by a modified commercial transient digitizer* that has a bandwidth of beyond 1 GHz and vertical sensitivity of 2 mV per division. For fast detectors with multiplication gains greater than 1×10^5, the external amplifier chain can be removed because the transient digitizer alone has sufficient sensitivity to display the single photoelectron pulses.

A trigger pulse from the countdown circuit is delayed to compensate for system delays and triggers the timebase used in the transient digitizer. This instrument digitizes low light level pulses, and the minicomputer processes the waveforms under program control.

For each waveform digitized, the peak pulse amplitude and total change are calculated by the analysis program in the minicomputer as shown in figure 6. Histograms of both the peak pulse amplitude and the total charge of each pulse are updated by the minicomputer for each waveform taken. Typical data runs

---

*The modification to the Tektronix R7912 transient digitizer was performed by the B&H Electronics Corporation and consisted of replacing the entire vertical channel of the digitizer with B&H 3000-series components.

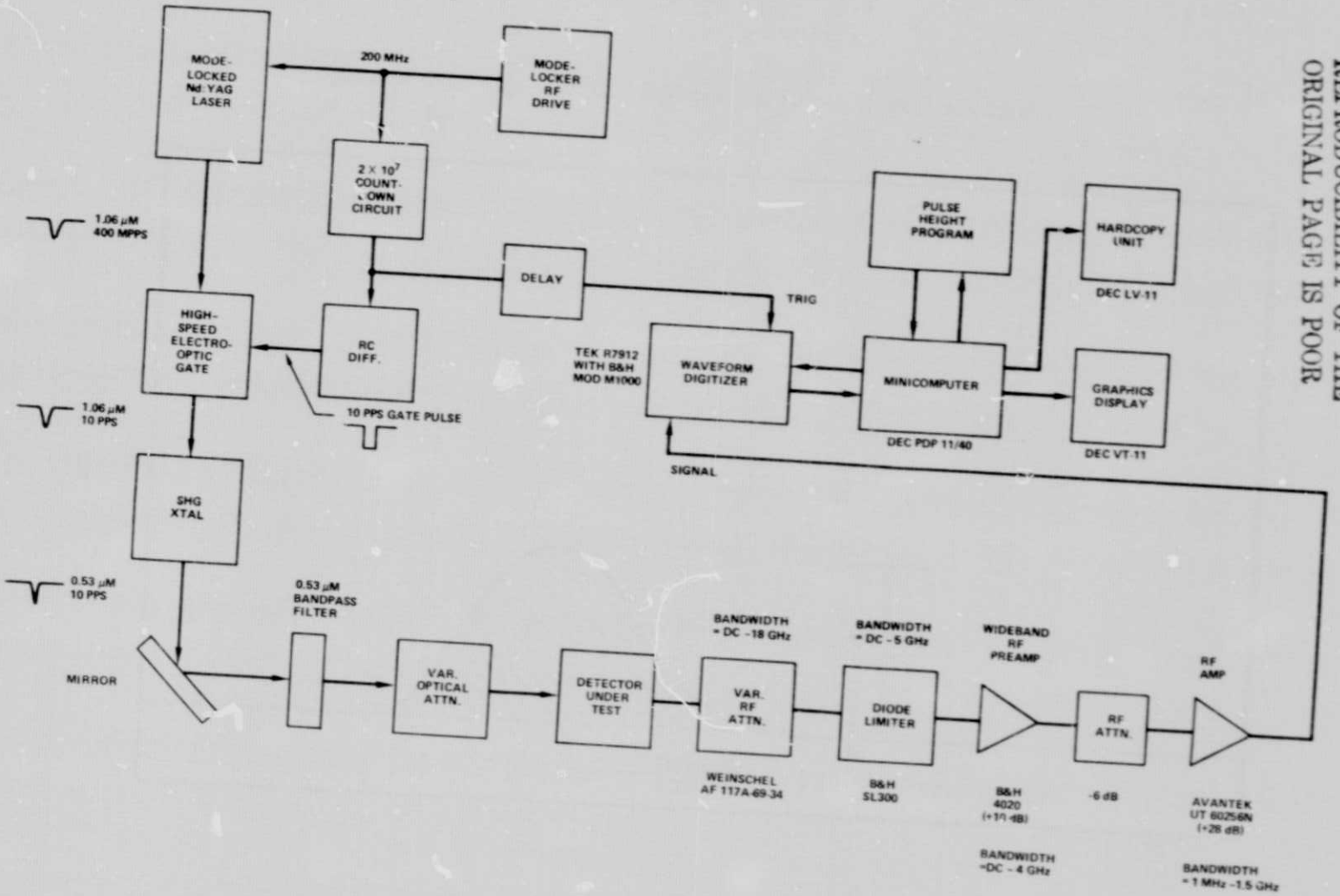

Figure 5. Block Diagram of System for Measuring Detector Pulse-height Spectrum

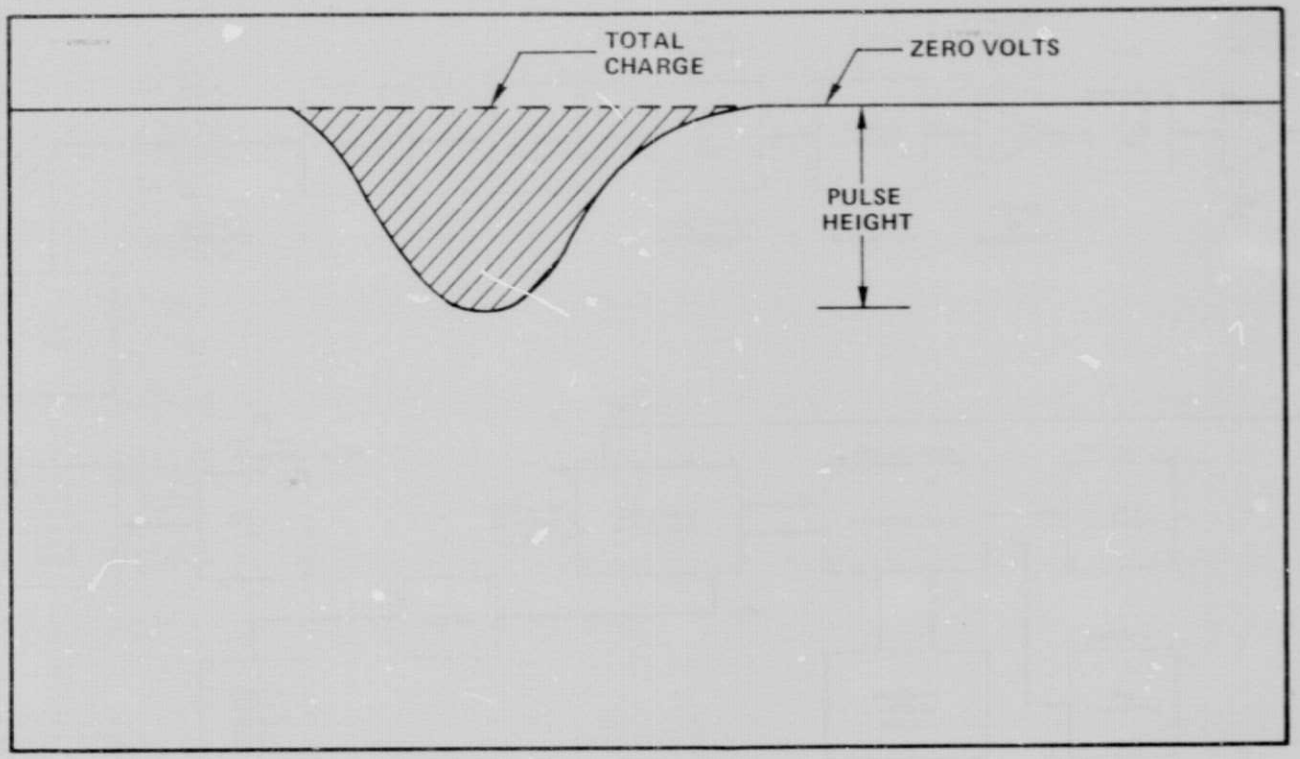

Figure 6. Waveform Analysis for Pulse Height Spectrum

are of 10,000 counts and are processed at a four waveform-per-second rate. The computer also updates an average waveform, which serves as a check for laser or measuring system drifts.

As a typical measurement, figure 7 shows low light level histogram for the static crossed-field photomultiplier. Both the peak and charge histograms show clearly resolved pulse peaks at the 1- and 2-photoelectron level. From this plot, the 1-photoelectron level of this detector was measured to be 6.5 mV, and the gain is measured to be 3.1×10^5. The similar shape of these two histograms indicates that the detector anode pulse had little width variation, since any pulse-width changes on a pulse-to-pulse basis would degrade the shape of the peak histogram.

The absolute position of the photoelectron peaks in the peak histogram is a function of measuring system bandwidth, since the measuring system risetime is much slower than the risetime of the static crossed-field detector. However, the peak in the total charge histogram is not affected by the measuring system bandwidth limitation, because, even under these conditions the total charge in the anode pulse is conserved.

Transit-Time Jitter Measurement

The time resolution of photomultipliers with GaP(Cs) dynodes has been the subject of recent analytical and experimental research.[20-24] For a typical measurement system described in these references, the test photomultiplier output was connected to one constant fraction discriminator, while either the

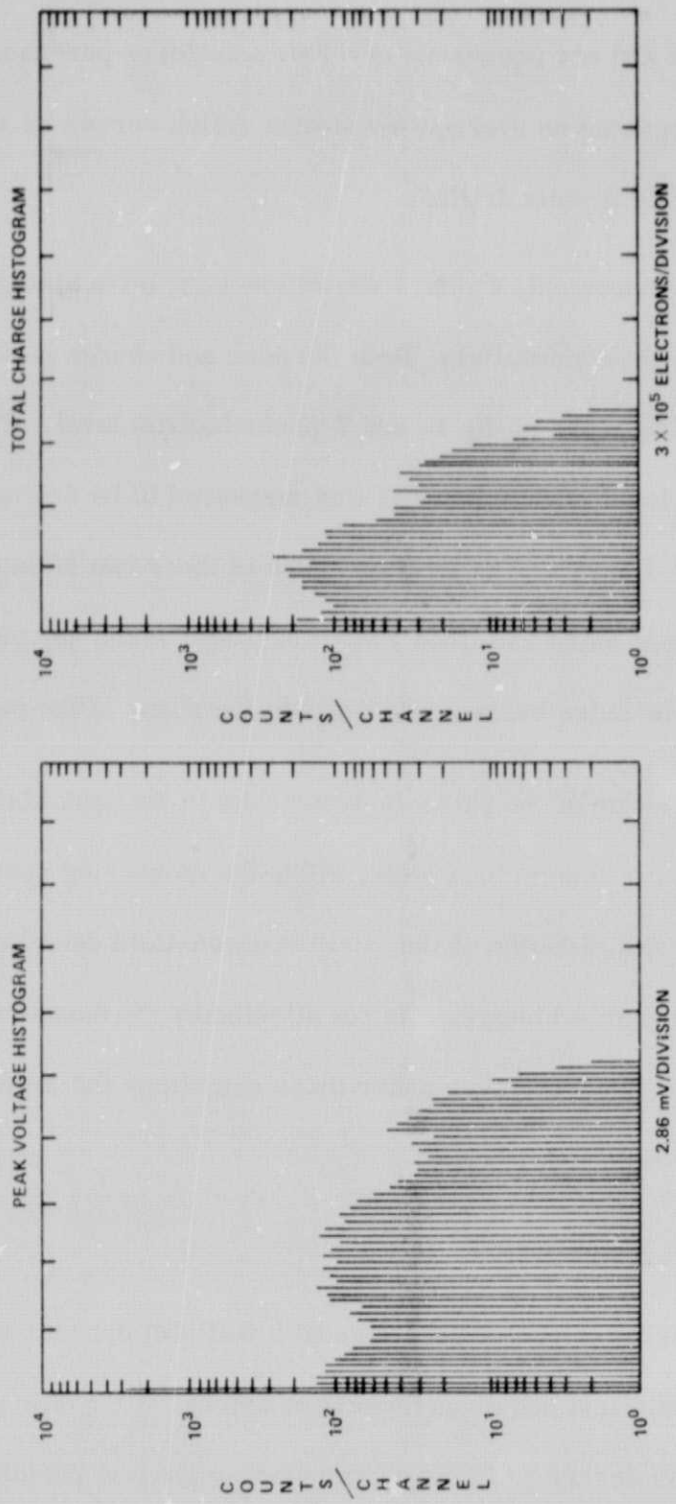

Figure 7. Pulse Height and Charge Spectra for Varian 154 A/1.6L No. 48

electrical pulse to a fast risetime light source or a reference photomultiplier output was connected to the other constant fraction discriminator. The time-to-pulse-height converter produced a pulse whose height is proportional to the time difference between the two discriminator firings. Distributions were accumulated by taking a large number of readings, usually when the test photomultiplier was detected signals of the 1-photoelectron level. Residual rms time jitters of as low as 34 ps have been reported for this measurement technique.[25]

Figure 8 shows the measurement system developed at GSFC. This system, which is based on measurements made using a fast transient digitizer, can resolve rms time jitters of 20 ps and average transit-time changes of 15 ps.

The laser, electro-optic gate, nonlinear optical crystal, optical bandpass filter, and amplifier chain are as in figure 5. The outgoing 0.53-μm pulse is split into two paths, with half the energy going to a low-gain low-jitter static crossed-field photomultiplier, and the remaining fraction going through an optical attenuator stack and then to the detector under test. The electrical output of the test detector is received by the amplifier chain, is electrically summed with the reference detector output by a matched 50-ohm power combiner, and is digitized by the transient digitizer. A representative waveform input to the transient digitizer is shown in figure 9.

The first pulse shown is the output from the reference detector; the second is from the test detector. For each detector tested, the electrical and optical

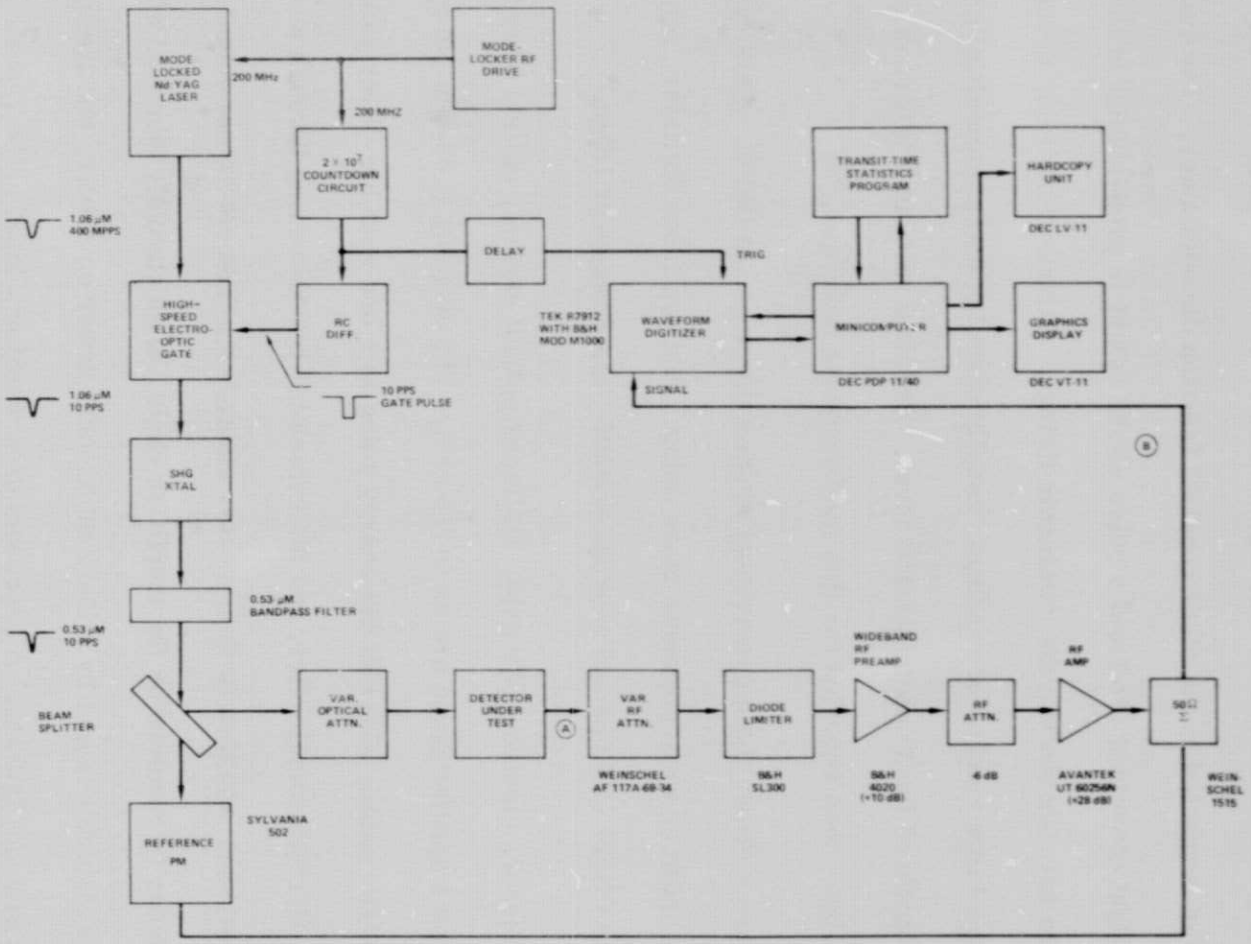

Figure 8. Block Diagram of System for Measuring Detector Transit Time Statistics

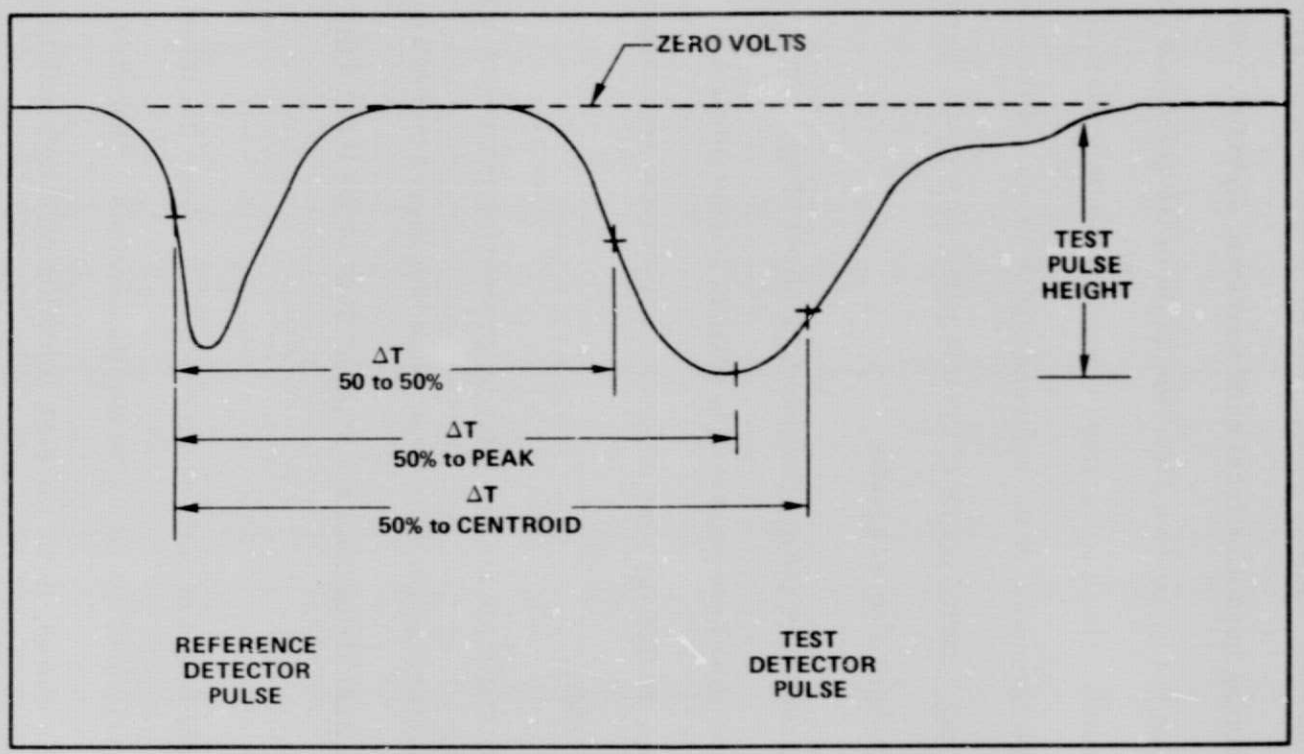

Figure 9. Waveform Analysis for Transit Time Statistics

delays of the system are adjusted to compensate for the fixed transit times of the test detector and the amplifier chain. The waveform analysis program measures three timing quantities from each waveform digitized, with each measurement using the 50-percent rise-time point of the reference pulse as a common timing point. These delta times consist of the time intervals beween the 50-percent risetime point of the reference pulse to each of the 50-percent risetime, peak, and centroid points of the test pulse as shown in figure 9. The test-pulse amplitude is also measured.

The use of a reference pulse eliminated the effect of any trigger jitter in the waveform digitizer time base because any random trigger jitter only delays the start of the sweep, so that the time difference between the reference and test pulses will not change.

Transit-time statistics are compiled by processing many such waveforms and building histograms of the delta-time valued measured on the waveform. Separate transit-time histograms are kept for each of the three detection strategies.

The test-pulse height of each waveform is used to sort the set of delta-time measurements into one of ten possible amplitude values. Therefore, a total of 30 histograms are stored, three for each detection strategy, with ten possible amplitude values for each strategy. During the data acquisition, the number of counts in each histogram is monitored, and the optical signal level to the test

detector is adjusted to obtain from 100 to 200 counts in each amplitude level. By analyzing this stored data with another minicomputer program, the mean value and standard deviation can be computed for each detection strategy at each amplitude level. As a result, the mean and standard deviation of transit time for each detection strategy can be plotted as a function of the test detector anode pulse amplitude.

To test the detector at higher signal levels, the gain of the amplifier chain can be reduced by adding electrical attenuation. By then removing optical attenuation, another data run can be made at this higher range of signal levels. In this way, the mean and rms time jitters of photomultipliers can be measured from the 1 to 1000 photoelectron range.

For calibration, a second low-gain static crossed-field photomultiplier was used as the test detector. The residual time jitter of the system was measured to be 17 ps. As a second calibration, the optical bandpass filter was removed, and 1.06-μm APD's were used for both the reference and the test detectors. For this case, the test detector was mounted on a translation base that had three fixed positions, each adding 6 mm to the optical path length. Each shift in APD position should therefore correspond to a measured time shift of 20 ps. For each APD position, the average transit time was measured as a function of the test APD peak output voltage, and the results are plotted in figure 10. As can be seen, the average transit-time curves show a $< \pm 10$-ps time walk over the measured amplitude range.

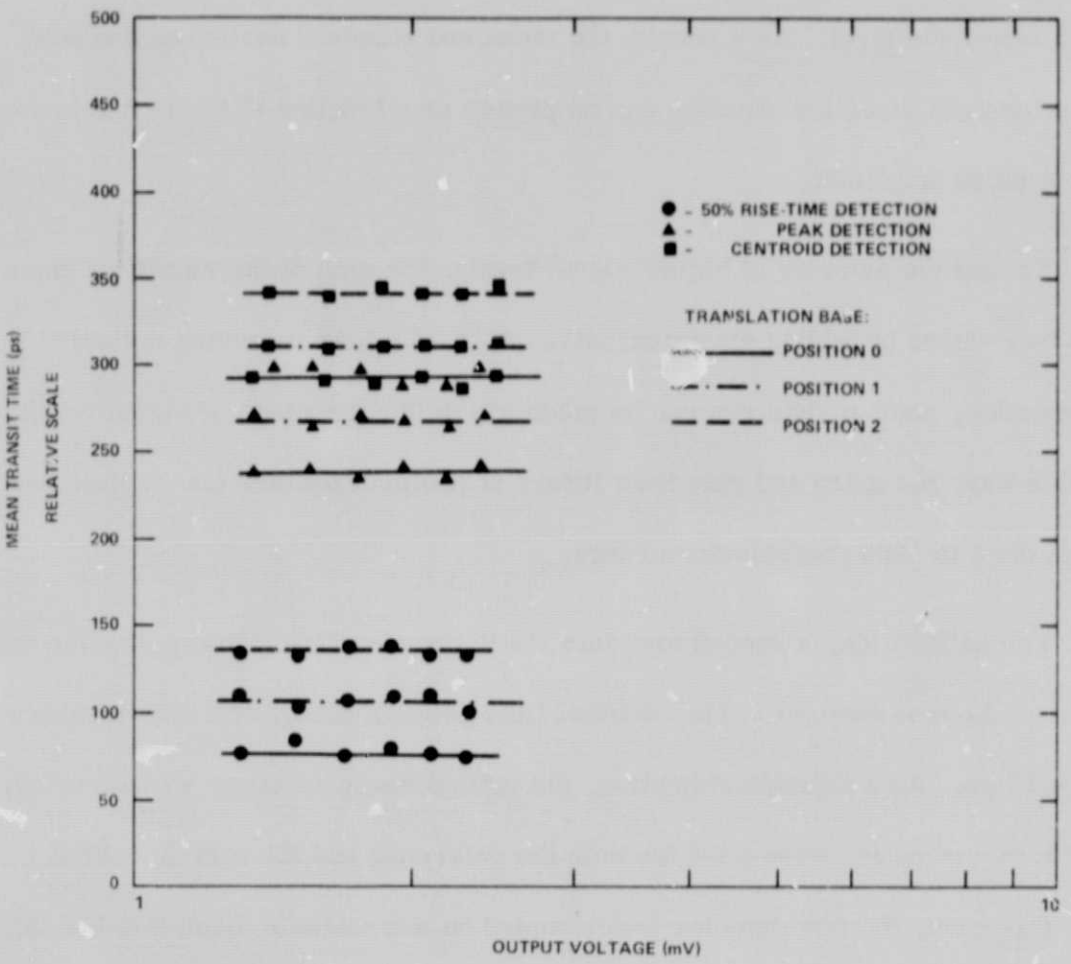

Figure 10. Mean Transit Time Versus Pulse Amplitude for 1.06 APD Time-Resolution Test with Detection Strategy as a Parameter

From figure 10, the average spacing between each successive detector position was measured to be 25 ps. The error between measured time shift and the actual time shift caused by the translation base is entirely the result of sweep-speed inaccuracies in the time base of the transient digitizer. This constant timing error was easily calibrated out of subsequent data analyses.

As typical measurement results, figure 11 shows the rms transit-time spread plotted versus signal level for the high-gain static crossed field photomultiplier. It shows the measured rms jitter to be less than 30 ps for the range of 1 to 100 photoelectrons. To the best of our knowledge, this is the lowest value reported for any photomultiplier. The mean transit time showed no measurable change over this signal range.

Dark-Count Spectrum

During testing of static crossed-field photomultipliers, large multiphotoelectron dark counts have been noted. These large dark counts are believed to originate from either photocathode bombardment from residual gas ions in the photomultiplier or cosmic-ray interaction with the photomultiplier window.[18] Measurements of the distribution of large dark counts are important because this internally generated noise places a lower limit on the false alarm rate of detection and ranging systems using these detectors.

Figure 12 shows the system used to measure this dark-count spectra. A tungsten bulb connected to a variable dc source provides a method for varying

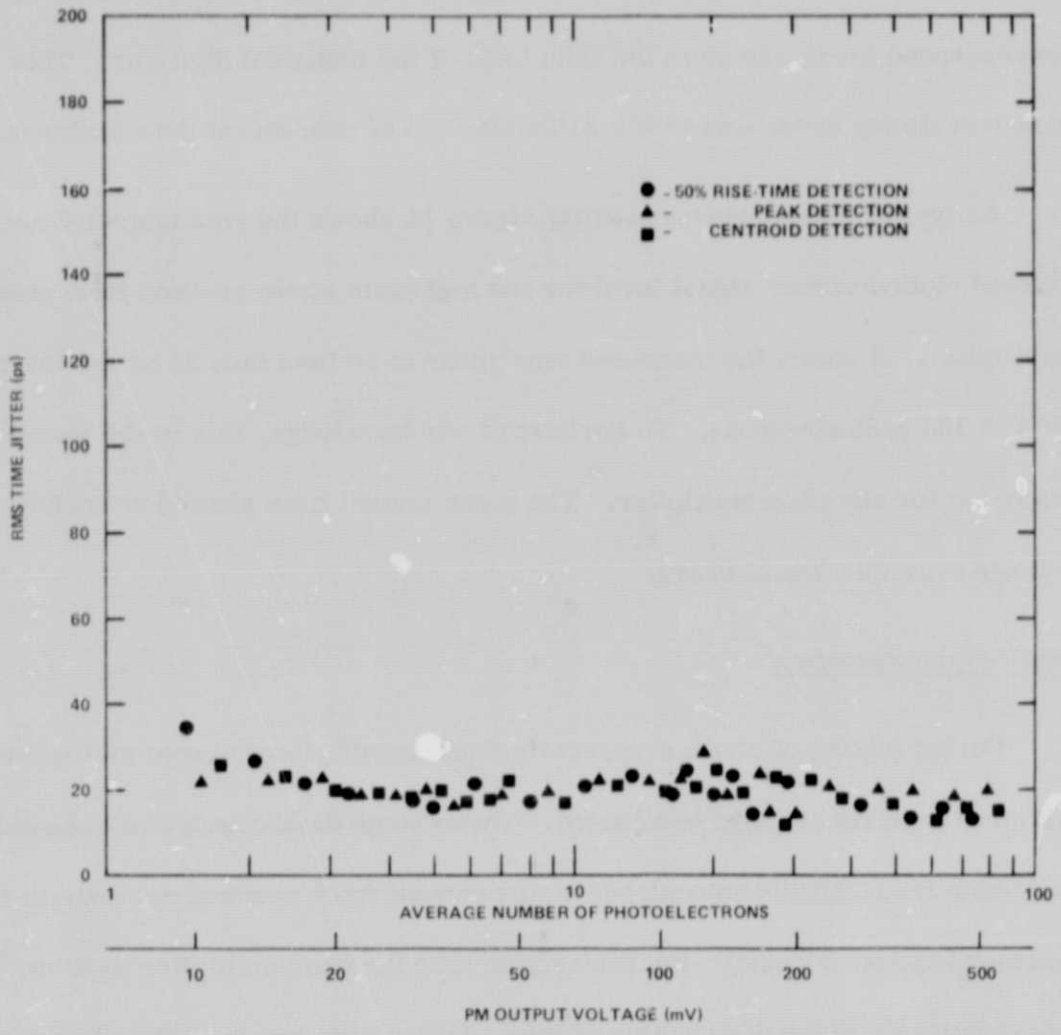

Figure 11. Rms Time Jitter Versus Pulse Amplitude for Varian 154 A/1.6L with Detection Strategy as a Parameter

Figure 12. Block Diagram of System for Measuring Dark-count Spectrum

the illumination on the photomultiplier photocathode. The output from the detector under test is switched either into a picoammeter to measure average anode current or into the amplifier chain described previously.

The output of the amplifier chain is connected to the fixed threshold discriminator which has a threshold of 70 ± 5 mV. The output pulses from this discriminator are counted by a frequency counter. By changing the electrical attenuator in the amplifier chain, the distribution of dark counts that exceed the threshold level can be measured. This measurement can in turn be repeated for different valued of average anode current. The resulting curves show the dark-count distribution for photomultipliers with continuous photocathode illumination using the average anode current as a parameter. As typical data, figure 13 shows the dark-count distributions for the static crossed-field photomultiplier. These distributions were measured with average anode currents of 5, 50, 500, 2000, and 10,000 nA. All curves show a sharp decrease in count rate in the 5- to 11-mV range, which corresponds to the single photoelectron emission range. Above this region, the dark-count spectrum does not change appreciably over the 2000:1 range in average anode current. This would suggest that the mechanism for producing the dark counts is independent of the average current through the photomultiplier.

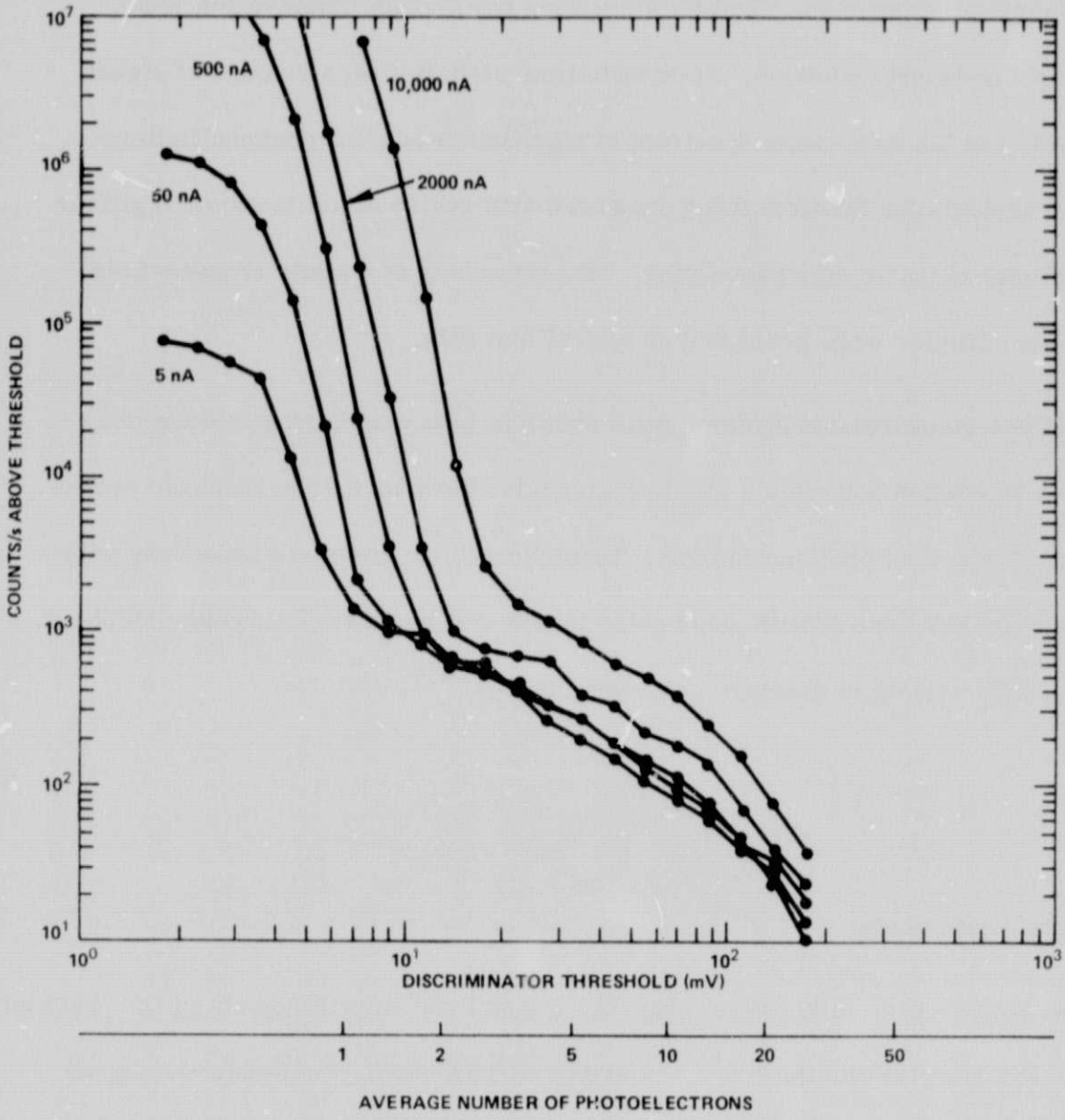

Figure 13. Noise Counts Versus Amplitude for Varian 154 A/1.6L with Average Anode Current as a Parameter

Conclusions

Systems have been described for measuring the average impulse response, the pulse-height spectrum, the transit-time statistics as a function of signal level, and the dark-count spectrum of gigahertz bandwidth photomultipliers. The systems for the first three measurements utilize a fast transient digitizer and minicomputer data processing. Measurements of a static crossed-field photomultiplier were presented as typical test data.

The new measurement systems were shown to have excellent amplitude and time resolution and offer a way to accurately characterize the response statistics of very fast photomultipliers. Such characterizations are necessary with the increasing use of both short pulse lasers and gigahertz bandwidth detectors in a wide variety of measurement systems.

Acknowledgments

The authors gratefully acknowledge the support and encouragement of Dr. Michael W. Fitzmaurice and the ready assistance of Thomas W. Zagwodzki during all phases of this work.

References

[1]B. Lescovar, C. L., P. Hartig, and K. Sauer, "Photon Counting System for Subnanosecond Fluorescence Lifetime Measurements," Lawrence Berkeley Laboratory, Engineering Note 4242, January 15, 1976.

[2]Melchoir, H., M. Fisher, and F. Arams, "Photodetectors for Optical Communication Systems, "Proceedings of the IEEE, 58 (10), 1970.

[3]McGunigal, T. E., W. J. Carrion, L. O. Candile, C. R. Grant, T. S. Johnson, D. A. Premo, P. L. Spadin, and G. C. Winston, "Satellite Laser Ranging Work at Goddard Space Flight Center," WESCON Technical Papers 19, Section 9/2, 1975.

[4]Anderson and B. McMurty, "High Speed Photodetectors, "Proceedings of the IEEE, 54 (10), October 1966.

[5]Vonbun, F. O., W. D. Kahn, P. D. Argentiero, D. W. Koch, K. J. Eng, "Spaceborne Earth Applications Ranging System (SPEAR), "NASA TM X71035, December 1975.

[6]J. B. Abshire and H. E. Rowe, "Characterization of Gigahertz Bandwidth Photomultipliers," NASA TM-78028, December 1977.

[7]Brookman, J. S., "Mode Locked Frequency Doubled Nd:YAG Laser," McDonnell Douglas Astronautics Corporation, Final Report for Contract NASS-20610, June 1976.

[8]Brand, J., "Optical Modulator System," McDonnell Douglas Astronautics Corporation, NASA CR-130195, October 1972.

[9]Pierce, J., and T. Paulus, Applied Electronics, Merrill, 1972, p. 528.

[10]Eder, R., "1.06 Micrometer Avalanche Photodiode Receiver," Rockwell International, NASA CR-144787, December 1975.

[11]Rabin, H., and C. Tang, Quantum Electronics, Vol. 1, Academic Press, 1975, p. 555.

[12]Rowe, H. E., and J. S. Osmundson, Measurements of Speed of Response of High Speed Visible and IR Optical Detectors, NASA TND-6874, August 1972.

[13]Simon, R. E., A. H. Sommer, J. J. Tietjen, and B. F. Williams, "New High Gain Dynode for Photomultipliers," Applied Physics Letters, 13 (10), 1968.

[14]Morton G., and H. Smith, "Pulse Height Resolution of High Gain First Dynode Photomultipliers," Applied Physics Letters, 13 (10), 1968.

[15]Prescot, J. R., "A Statistical Model for Photomultiplier Single Electron Statistics," Nuclear Instrumentation and Methods, 39 (9), 1966, pp. 173-179.

[16]Dietz, L. A., "Use of Poya Statics in Investigations of Electron Yields from Target Surfaces," Rev. Sci. Instr., 38 (9), 1967, pp. 1332-1333.

[17]Donati, S., E. Gatti, and V. Svelto, "Statistical Behavior of Scintillation Detector: Theories and Experiments," Advances in Electronics and Electron Physics, 26, 1968, p. 251.

[18]Morton, G. A., H. M. Smith, and H. R. Krall, "Performance of High Gain First Dynode Photomultipliers," IEEE Transactions on Nuclear Science, NS-16 (1), 1969, p. 92.

[19]Krall, H. R., F. A. Helny, and D. E. Persyk, "Recent Developments in GaP(Cs)—Dynode Photomultipliers," IEEE Transactions on Nuclear Science, NS-17 (3), 1970, p. 71.

[20]Lescovar, B., and C. Lo, "Performance Studies of Photomultipliers Having Dynodes with GaP (Cs) Secondary Emitting Surface," IEEE Transactions on Nuclear Science, 19 (3), 1972, p. 50.

[21]Krall, H., and D. Persyk, "Recent Work on Fast Photomultipliers Utilizing GaP(Cs) Dynodes," IEEE Transactions on Nuclear Science, NS-19 (3), 1972, p. 45.

[22]Reisse, R., R. Cressy, and S. K. Poultney, "Single Photon Detection and Subnanosecond Timing Resolution with the RCA C313034 Photomultiplier," Rev. Sci. Instr., 44 (11), 1973.

[23]Miehe, J., G. Ambard, J. Zampach, and A. Coche, "Statistics and Timing of the First Photoelectron with a High Gain Dynode Photomultiplier," IEEE Transactions on Nuclear Science, NS-17 (3), 1970, p. 115.

[24]Broll, N., B. Sipp, and J. A. Miehe, "Single Electron Response of Fast Photomultipliers," IEEE Transactions on Nuclear Sciences, NS-21 (12), 1974.

[25]Lo, C., and B. Lescovar, "A Measuring System for Studying the Time Resolution Capabilities of Fast Photomultipliers," IEEE Transactions on Nuclear Science, NS-21 (1), 1974, p. 93.